

Platinum Metal Complexes of Potentially Chelating Alkene–Sulphur and Alkene–Selenium Ligands. The Synthesis by Chalcogen Dealkylation and X-Ray Structures of the Dimeric Complexes $[\{\text{Pt}(\text{SCH}_2\text{CH}_2\text{CMe}=\text{CH}_2)\}_2]$ and $[\{\text{Pt}(\text{PPh}_3)(\text{SCH}_2\text{CH}_2\text{CMe}=\text{CH}_2)\}_2]$,† and a Dynamic Nuclear Magnetic Resonance Study of $[\{\text{Pt}(\text{L})(\text{SCH}_2\text{CH}_2\text{CMe}=\text{CH}_2)\}_2]$ [L = PPh₃, PPh₂Me, or As(CH₂SiMe₃)₃]

Edward W. Abel, David G. Evans,* and Julian R. Koe
Department of Chemistry, University of Exeter, Exeter EX4 4QD

Michael B. Hursthouse and Mohammed Mazid
Department of Chemistry, Queen Mary College, London E1 4NS

Mary F. Mahon and Kieran C. Molloy
School of Chemistry, University of Bath, Claverton Down, Bath BA2 7AY

The chelating ligands 2,8-dimethyl-5-thianona-1,8-diene and 2,8-dimethyl-5-selenanona-1,8-diene have been found to undergo unusually facile chalcogen dealkylation on treatment with halide when co-ordinated to platinum(II). The resulting dimeric complexes contain chelating bridging alkenyl thiolato and alkenyl selenato ligands and have been fully characterised. An X-ray diffraction study of $[\{\text{Pt}(\text{SCH}_2\text{CH}_2\text{CMe}=\text{CH}_2)\}_2]$ is reported: the crystals are orthorhombic, space group *Pbca* with *Z* = 1 in a unit cell of dimensions *a* = 12.733(3), *b* = 15.288(2), and *c* = 16.904(3) Å. The molecular structure involves a non-planar Pt₂S₂ ring, with square-planar co-ordination at each platinum being completed by the chelating alkene and iodide ligands. The principal internuclear distances are Pt(1)–I(1) 2.624(2), Pt(2)–I(2) 2.621(2), Pt(1)–S(1) 2.295(6), Pt(1)–S(2) 2.330(6), Pt(2)–S(1) 2.334(6), Pt(2)–S(2) 2.304(6), Pt(1)–C 2.216(25) and 2.21(3), Pt(2)–C 2.207(24) and 2.155(23) Å. The co-ordinated alkene functions are displaced by ligands containing Group 5A donor atoms yielding dimeric complexes which contain non-chelating bridging alkenyl thiolato and alkenyl selenato ligands and which have been fully characterised. Inversion of configuration at the bridging chalcogen atom is observed at moderate temperatures and has been studied by dynamic n.m.r. spectroscopy. An X-ray diffraction study of $[\{\text{Pt}(\text{PPh}_3)(\text{SCH}_2\text{CH}_2\text{CMe}=\text{CH}_2)\}_2]$ is reported: the crystals are triclinic, of space group *P* $\bar{1}$, with *Z* = 1 in a unit cell of dimensions *a* = 10.396(1), *b* = 11.250(5), and *c* = 13.348(2) Å with α = 91.63(3)°, β = 94.53(1)°, and γ = 116.02(3)°. The molecular structure involves a planar Pt₂S₂ ring, with square-planar co-ordination at each platinum being completed by triphenylphosphine and iodide ligands. The molecule has a centre of inversion. The principal internuclear distances are Pt–I 2.621(1), Pt–S 2.367(3), and Pt–P 2.267(3) Å.

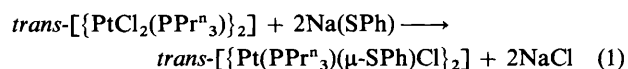
Continuing our studies on transition-metal complexes of potentially chelating ligands containing both an alkenyl moiety and a chalcogen atom which have hitherto involved monoalkenyl chalcogenoethers¹ and dialkenylchalcogenoethers,² we now report the synthesis of dimeric complexes containing either chelating or non-chelating bridging alkenyl thiolato and alkenyl selenato ligands [Type (1) and (2), respectively].

Thiolato-bridged complexes have long been known,^{3,4} the presence of the Pt₂S₂ ring conferring considerable stability upon these compounds. In contrast to thioether ligands which readily form terminal complexes, the thiolato group favours bridged complexes, stemming from the fact that it is highly polarisable and has an additional lone pair.⁴ The stability of such bridged dimeric thiolato complexes is illustrated by their unreactivity towards methyl iodide and monodentate ligands such as pyridine and triphenylphosphine,⁵ although some oligomeric thiolato-bridged compounds may be cleaved using very strongly co-ordinating ligands such as dimethylphenylphosphine.⁶

Due to the pyramidal nature of the chalcogen atom, thiolato- and selenato-bridged complexes may exist in several isomeric forms which may interconvert by the intramolecular fluxional processes of pyramidal atomic inversion, first recorded for sulphur in transition-metal complexes in 1966,^{7,8} and also ring

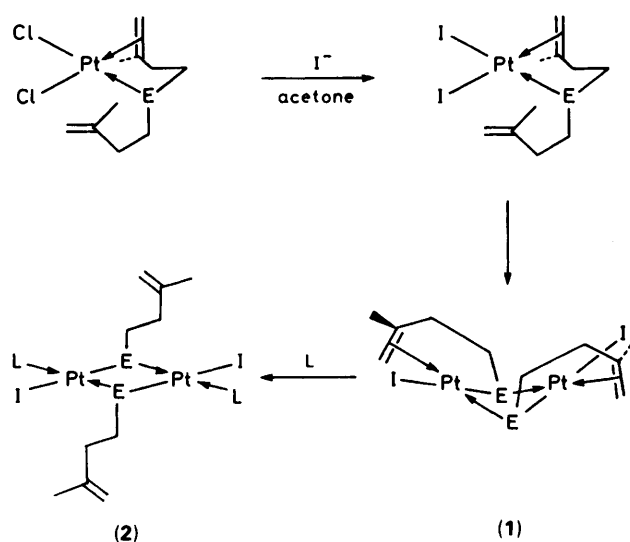
reversal. The rate of chalcogen inversion depends very much upon the environment of the inverting centre, but it is generally true that the energy barrier to inversion is less in the case of sulphur than that of selenium,⁹ and also that inversion occurs more easily in bridging thiolato- and selenato-complexes than in terminal thioether and selenoether complexes. The ease of chalcogen inversion in bridging chalcogenato complexes of RE[–] ligands (E = S or Se) also depends upon the nature of the group R: a larger R group favours a lower free energy of activation for the inversion process.

The synthesis of thiolato-bridged platinum(II) and palladium(II) dinuclear complexes is usually accomplished by the replacement of terminal and/or bridging chloride ligands by the RS[–] group, furnished from the thiol,¹⁰ as in equation (1). A



† Bis(μ-3-methylbut-3-enethiolato-C^{3,4}, μ-S)-bis[iodoplatinum(II)] and bis(μ-3-methylbut-3-enethiolato-S)-bis[iodo(triphenylphosphine)-platinum(II)].

Supplementary data available: see Instructions for Authors, *J. Chem. Soc., Dalton Trans.*, 1990, Issue 1, pp. xix–xxii.



Scheme 1. E = S or Se, L = PPh₃, PPh₂Me, or As(CH₂SiMe₃)₃

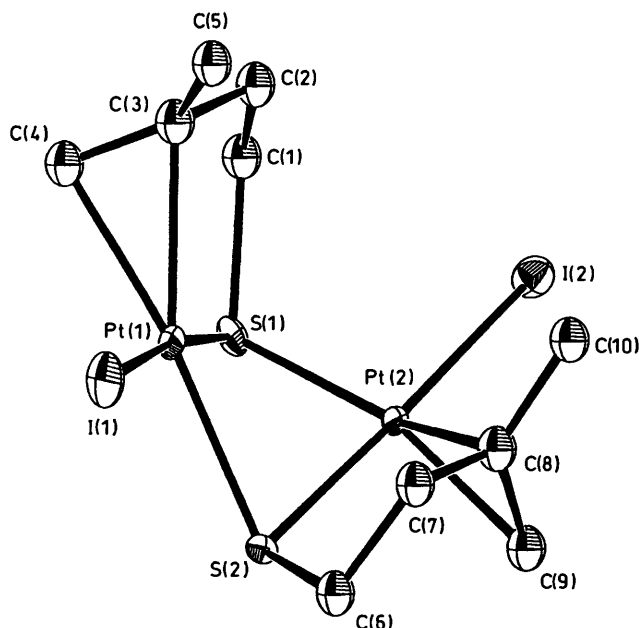
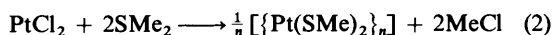


Figure 1. Molecular structure of $[\{\text{PtI}(\text{SCH}_2\text{CH}_2\text{CMe}=\text{CH}_2)\}_2]_2$, illustrating the folded nature of the complex

more unusual and less generally applicable route is by chalcogen dealkylation (*i.e.* alkyl-chalcogen cleavage of one of the S/Se-C bonds in chalcogenoethers). S-Dealkylation was first reported in 1883¹¹ when the S-demethylation of dimethyl sulphide by PtCl₂ was observed as in equation (2).



Alkyl-thio cleavage in dimeric platinum(II) complexes is usually effected only under forcing conditions by refluxing the complex with halide ions in a high-boiling polar solvent such as dimethylformamide. Reaction is envisaged as S_N2 attack by the halide ion on the carbon atom (α to sulphur) of the group to be removed.¹²

We now report particularly facile S- and Se-dealkylation of *cis*-(2,8-dimethyl-5-chalcogenanona-1,8-diene)dihalogeno-

platinum(II), $[\text{PtX}_2\{\text{E}(\text{CH}_2\text{CH}_2\text{CMe}=\text{CH}_2)_2\}]$ (X = Cl, Br, or I; E = S or Se), to yield dimeric complexes bridged by chelating alkenyl-thiolato and -selenato ligands $[\{\text{PtX}(\text{ECH}_2\text{CH}_2\text{CMe}=\text{CH}_2)\}_2]$. We report also the displacement of the coordinated alkene moiety by various ligands containing Group 5A donor atoms and a study of chalcogen inversion in the resulting complexes of the type $[\{\text{PtI}(\text{ECH}_2\text{CH}_2\text{CMe}=\text{CH}_2)\text{L}\}_2]$ [E = S or Se; L = PPh₃, PPh₂Me, or As(CH₂SiMe₃)₃].

Results and Discussion

Preparation and Properties of the Complexes.—The complexes $[\{\text{PtX}(\text{ECH}_2\text{CH}_2\text{CMe}=\text{CH}_2)\}_2]$ (1) (X = Cl, Br, or I; E = S or Se) containing chelating alkenyl-thiolato and -selenato ligands were synthesised by alkyl-chalcogen cleavage (see Scheme 1) of the dialkenylchalcogenoether ligand² co-ordinated to the platinum(II) centre in the complexes $[\text{PtX}_2\{\text{E}(\text{CH}_2\text{CH}_2\text{CMe}=\text{CH}_2)_2\}]$ ² and subsequent dimerisation of the two metal moieties. The reaction occurred on refluxing an acetone solution of the complex with *ca.* 3 equivalents of the appropriate lithium halide (X = Br or I) (to encourage S_N2 attack in the dealkylation process). The complexes $[\{\text{PtI}(\text{L})(\text{ECH}_2\text{CH}_2\text{CMe}=\text{CH}_2)\}_2]$ (2) [L = PPh₃, PPh₂Me, or As(CH₂SiMe₃)₃] containing non-chelating alkenyl-thiolato and -selenato ligands were synthesised by displacing the alkene moieties in the complexes $[\{\text{PtI}(\text{ECH}_2\text{CH}_2\text{CMe}=\text{CH}_2)\}_2]$ with 2 equivalents of the ligand L in chloroform at room temperature. The complexes are all crystalline, of moderate to good solubility in chlorocarbon solvents, and stable to air and water as solids and in solution. Infrared and analytical data are reported in Tables 1 and 2, respectively. The complexes have been further characterised by variable-temperature n.m.r. spectroscopy and for $[\{\text{PtI}(\text{SCH}_2\text{CH}_2\text{CMe}=\text{CH}_2)\}_2]$ and $[\{\text{PtI}(\text{PPh}_3)(\text{SCH}_2\text{CH}_2\text{CMe}=\text{CH}_2)\}_2]$ by single-crystal X-ray diffraction. The infrared and n.m.r. studies clearly show whether the bridging chalcogenato ligands chelate through the alkene moiety or whether the latter remains unco-ordinated. Variable-temperature n.m.r. studies on the complexes $[\{\text{PtI}(\text{L})(\text{ECH}_2\text{CH}_2\text{CMe}=\text{CH}_2)\}_2]$ [L = PPh₃, PPh₂Me, or As(CH₂SiMe₃)₃; E = S or Se] indicate the occurrence of configurational inversion at sulphur and selenium and quantitatively demonstrate the effects of the different chalcogen atoms and the different ligands, L. The n.m.r. studies on these complexes also indicate the occurrence in solution of a much slower process: that of *trans* to *cis* isomerisation of the terminal ligands.

In order to provide a starting point for the discussion of the solution-state behaviour it was desirable to know the structures of complexes in the solid state and hence single-crystal X-ray analyses were undertaken for one dimer of each type. The relevant details are given in the Experimental section.

Crystal and Molecular Structure of $[\{\text{PtI}(\text{SCH}_2\text{CH}_2\text{CMe}=\text{CH}_2)\}_2]_2$.—The molecular structure of the complex is illustrated in Figure 1 and selected intramolecular bond lengths and angles are given in Table 3. The fractional atomic co-ordinates are given in Table 4. The molecule has a non-planar 'open-book' structure generated by approximately square-planar co-ordination about the two platinum atoms (described by the iodine atom, the two sulphur atoms, and the centroid of the alkene double bond) and pyramidal geometry at the two sulphur atoms. The alkene moiety is bound transversely to the square-planar co-ordination sphere of the metal as is normal in *d*⁸ metal-alkene complexes.¹³ The molecule has a non-crystallographic C₂ axis.

The fold angle between the two square-planar platinum(II) moieties at the midpoint of the S...S vector is 115.6°. The observed hinge angle in folded complexes of the type $[\text{Pt}_2(\mu\text{-SR})_2\text{X}_2\text{L}_2]$ generally¹⁴ lies in the range 130–141° and the small

Table 1. Infrared data (cm^{-1}), KBr discs unless stated otherwise

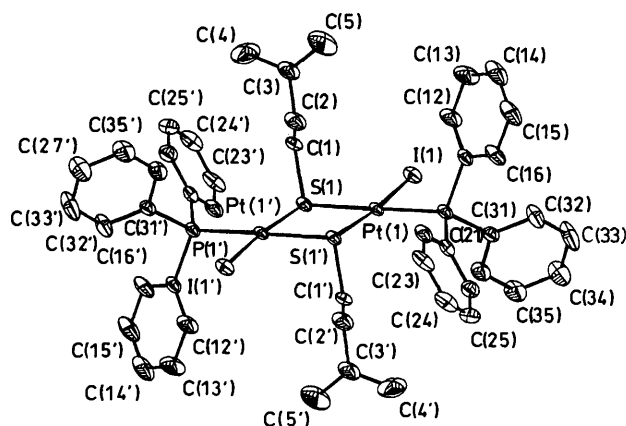
Sample	Alkene stretch	
	Unco-ordinated	Co-ordinated
$\text{S}(\text{CH}_2\text{CH}_2\text{CMe}=\text{CH}_2)_2^*$	1 650	
$\text{Se}(\text{CH}_2\text{CH}_2\text{CMe}=\text{CH}_2)_2^*$	1 647	
$[\text{PtCl}_2\{\text{S}(\text{CH}_2\text{CH}_2\text{CMe}=\text{CH}_2)_2\}]_2$	1 648	1 511
$[\text{PtBr}_2\{\text{S}(\text{CH}_2\text{CH}_2\text{CMe}=\text{CH}_2)_2\}]_2$	1 650	1 514
$[\text{PtI}_2\{\text{S}(\text{CH}_2\text{CH}_2\text{CMe}=\text{CH}_2)_2\}]_2$	1 647	1 512
$[\text{PtCl}_2\{\text{Se}(\text{CH}_2\text{CH}_2\text{CMe}=\text{CH}_2)_2\}]_2$	1 647	1 510
$[\text{PtBr}_2\{\text{Se}(\text{CH}_2\text{CH}_2\text{CMe}=\text{CH}_2)_2\}]_2$	1 644	1 508
$[\{\text{PtCl}(\text{SCH}_2\text{CH}_2\text{CMe}=\text{CH}_2)_2\}]_2$		1 509
$[\{\text{PtBr}(\text{SCH}_2\text{CH}_2\text{CMe}=\text{CH}_2)_2\}]_2$		1 507
$[\{\text{PtI}(\text{SCH}_2\text{CH}_2\text{CMe}=\text{CH}_2)_2\}]_2$		1 511
$[\{\text{PtCl}(\text{SeCH}_2\text{CH}_2\text{CMe}=\text{CH}_2)_2\}]_2$		1 514
$[\{\text{PtBr}(\text{SeCH}_2\text{CH}_2\text{CMe}=\text{CH}_2)_2\}]_2$		1 506
$[\{\text{PtI}(\text{SeCH}_2\text{CH}_2\text{CMe}=\text{CH}_2)_2\}]_2$		1 505
$[\{\text{PtI}(\text{PPh}_3)(\text{SCH}_2\text{CH}_2\text{CMe}=\text{CH}_2)_2\}]_2$	1 645	
$[\{\text{PtI}[\text{As}(\text{CH}_2\text{SiMe}_3)_3](\text{SCH}_2\text{CH}_2\text{CMe}=\text{CH}_2)_2\}]_2$	1 647	
$[\{\text{PtI}(\text{PPh}_3)(\text{SeCH}_2\text{CH}_2\text{CMe}=\text{CH}_2)_2\}]_2$	1 641	
$[\{\text{PtI}[\text{As}(\text{CH}_2\text{SiMe}_3)_3](\text{SeCH}_2\text{CH}_2\text{CMe}=\text{CH}_2)_2\}]_2$	1 647	

* Liquid film.

Table 2. Characterisation of the crystalline complexes

Complex	Colour	M.p./ $^{\circ}\text{C}$	Analysis* /%	
			C	H
$[\{\text{PtCl}(\text{SCH}_2\text{CH}_2\text{CMe}=\text{CH}_2)_2\}]_2$	Orange	250 (decomp.)	18.40 (18.10)	2.70 (2.75)
$[\{\text{PtBr}(\text{SCH}_2\text{CH}_2\text{CMe}=\text{CH}_2)_2\}]_2$	Orange	202 (decomp.)	16.15 (15.95)	2.30 (2.40)
$[\{\text{PtI}(\text{SCH}_2\text{CH}_2\text{CMe}=\text{CH}_2)_2\}]_2$	Dark red	200 (decomp.)	14.25 (14.20)	2.00 (2.15)
$[\{\text{PtCl}(\text{SeCH}_2\text{CH}_2\text{CMe}=\text{CH}_2)_2\}]_2$	Orange	220 (decomp.)	15.85 (15.85)	2.40 (2.40)
$[\{\text{PtBr}(\text{SeCH}_2\text{CH}_2\text{CMe}=\text{CH}_2)_2\}]_2$	Red	218 (decomp.)	14.15 (14.20)	2.00 (2.15)
$[\{\text{PtI}(\text{SeCH}_2\text{CH}_2\text{CMe}=\text{CH}_2)_2\}]_2$	Dark mauve	185 (decomp.)	12.85 (12.80)	1.70 (1.95)
$[\{\text{PtI}(\text{PPh}_3)(\text{SCH}_2\text{CH}_2\text{CMe}=\text{CH}_2)_2\}]_2 \cdot \text{CHCl}_3$	Yellow	217	36.75 (37.90)	3.20 (3.30)
$[\{\text{PtI}[\text{As}(\text{CH}_2\text{SiMe}_3)_3](\text{SCH}_2\text{CH}_2\text{CMe}=\text{CH}_2)_2\}]_2$	Yellow	181–182	26.90 (26.90)	5.60 (5.55)
$[\{\text{PtI}(\text{PPh}_3)(\text{SeCH}_2\text{CH}_2\text{CMe}=\text{CH}_2)_2\}]_2 \cdot \text{CHCl}_3$	Yellow	191	34.25 (34.90)	2.95 (3.05)
$[\{\text{PtI}[\text{As}(\text{CH}_2\text{SiMe}_3)_3](\text{SeCH}_2\text{CH}_2\text{CMe}=\text{CH}_2)_2\}]_2$	Yellow	191	25.40 (25.30)	5.15 (5.25)

* Calculated values in parentheses.

**Figure 2.** Molecular structure of $[\{\text{PtI}(\text{PPh}_3)(\text{SCH}_2\text{CH}_2\text{CMe}=\text{CH}_2)_2\}]_2$, illustrating the planar nature of complex

value in this case is a consequence of constraints imposed by chelation of the ligand. This fold brings the two platinum atoms to within a short distance [$3.024(1) \text{ \AA}$] of each other compared with literature¹⁴ values ($3.18\text{--}3.34 \text{ \AA}$), but although some interaction between them is possible its extent is likely to be small but might perhaps account for the unusually intense colours of the complexes. A similar folding in a dimeric nickel

complex containing chelating bridging thiolate ligands, $[\{\text{Ni}(\mu\text{-SCH}_2\text{CH}_2\text{NHCH}_2\text{CH}_2\text{-}o\text{-C}_5\text{H}_4\text{N})_2\}]^{2+}$, has been observed,¹⁵ with a fold angle of 110° . This allows the nickel atoms to approach each other to a distance of $2.739(1) \text{ \AA}$, where some metal-metal interaction is also possible.

The platinum-sulphur bond lengths in the complex are in the range expected¹⁴ but differ significantly, demonstrating their sensitivity to the *trans* influence of the *trans* ligand. The Pt-S bond lengths *trans* to the alkene [$2.334(6)$ and $2.330(6) \text{ \AA}$] are longer than those *trans* to iodide [$2.295(6)$ and $2.304(6) \text{ \AA}$], consistent with the greater *trans* influence of alkene compared with halogen.

Crystal and Molecular Structure of $[\{\text{PtI}(\text{PPh}_3)(\text{SCH}_2\text{CH}_2\text{CMe}=\text{CH}_2)_2\}]_2$.—The molecular structure of this complex is illustrated in Figure 2 and selected intramolecular bond lengths and angles are given in Table 5. The fractional atomic coordinates are given in Table 6.

The structure differs from that of its precursor in that the Pt-S-Pt-S ring is planar, and the molecule has a centre of inversion. The co-ordination geometry about each platinum atom is again square planar with the two bridging sulphur atoms occupying mutually *cis* positions and the other two sites being occupied by iodine and triphenylphosphine. The bridging sulphur atoms also retain a pyramidal geometry, but since the bridging ligands no longer impose particular geometric con-

Table 3. Selected intramolecular bond lengths (Å) and angles (°) for $[\{\text{Pt}(\text{SCH}_2\text{CH}_2\text{CMe}=\text{CH}_2)\}_2]$

Pt(1)–S(1)	2.295(6)	Pt(1)–I(1)	2.624(2)
Pt(1)–C(1)	3.22(3)	Pt(1)–S(2)	2.330(6)
Pt(1)–C(3)	2.216(25)	Pt(1)–C(2)	3.03(3)
Pt(1)–C(5)	3.11(3)	Pt(1)–C(4)	2.21(3)
Pt(2)–S(1)	2.334(6)	Pt(2)–I(2)	2.621(2)
Pt(2)–C(6)	3.184(23)	Pt(2)–S(2)	2.304(6)
Pt(2)–C(8)	2.207(24)	Pt(2)–C(7)	2.98(3)
Pt(2)–C(10)	3.10(3)	Pt(2)–C(9)	2.155(23)
S(1)–C(1)	1.83(3)	S(2)–C(6)	1.831(24)
C(1)–C(2)	1.48(4)	C(2)–C(3)	1.54(3)
C(3)–C(4)	1.40(4)	C(3)–C(5)	1.50(4)
C(6)–C(7)	1.49(4)	C(7)–C(8)	1.51(3)
C(8)–C(9)	1.50(3)	C(8)–C(10)	1.44(4)
S(1)–Pt(1)–I(1)	173.3(2)	S(2)–Pt(1)–S(2)	179.3(2)
S(2)–Pt(1)–I(1)	94.4(2)	C(3)–Pt(1)–S(1)	86.6(6)
C(3)–Pt(1)–I(1)	100.0(6)	C(4)–Pt(1)–S(1)	92.5(8)
C(3)–Pt(1)–S(2)	151.2(6)	S(2)–Pt(2)–S(1)	79.0(2)
C(4)–Pt(1)–I(1)	93.2(8)	C(8)–Pt(2)–S(1)	148.4(6)
C(4)–Pt(1)–S(2)	166.2(9)	C(9)–Pt(2)–S(1)	165.0(6)
S(1)–Pt(2)–I(2)	95.8(2)	C(9)–Pt(2)–C(8)	40.3(9)
S(2)–Pt(2)–I(2)	173.6(2)	C(1)–S(1)–Pt(1)	101.9(9)
C(8)–Pt(2)–I(2)	99.3(6)	C(6)–S(2)–Pt(1)	111.8(8)
C(8)–Pt(2)–S(2)	87.0(6)	C(3)–C(2)–C(1)	117(2)
C(9)–Pt(2)–I(2)	92.9(6)	C(4)–C(3)–Pt(1)	71(2)
C(9)–Pt(2)–S(2)	91.3(6)	C(5)–C(3)–Pt(1)	112(2)
Pt(2)–S(1)–Pt(1)	81.6(2)	C(5)–C(3)–C(4)	122(2)
C(1)–S(1)–Pt(2)	111.9(9)	C(8)–C(7)–C(6)	116(2)
Pt(2)–S(2)–Pt(1)	81.5(2)	C(9)–C(8)–Pt(2)	68(1)
C(6)–S(2)–Pt(2)	100.1(8)	C(10)–C(8)–Pt(2)	115(2)
C(2)–C(1)–S(1)	110(2)	C(10)–C(8)–C(9)	122(2)
C(2)–C(3)–Pt(1)	106(2)	C(8)–C(10)–Pt(2)	40(1)
C(4)–C(3)–C(2)	123(2)	C(5)–C(3)–C(2)	112(2)
C(3)–C(4)–Pt(1)	72(2)	C(7)–C(6)–S(2)	109(2)
C(7)–C(8)–Pt(2)	105(2)	C(9)–C(8)–C(7)	120(2)
C(10)–C(8)–C(7)	114(2)	C(8)–C(9)–Pt(2)	72(1)

Table 4. Fractional atomic co-ordinates for $[\{\text{PtI}(\text{SCH}_2\text{CH}_2\text{CMe}=\text{CH}_2)\}_2]$

Atom	x	y	z
Pt(1)	0.151 87(8)	0.209 33(6)	0.076 66(5)
Pt(2)	0.222 82(7)	0.098 43(6)	0.215 08(5)
I(1)	0.163 54(2)	0.169 02(1)	–0.074 02(1)
I(2)	0.120 15(15)	0.056 93(14)	0.344 14(10)
S(1)	0.162 59(5)	0.243 04(4)	0.208 75(4)
S(2)	0.315 52(5)	0.150 14(4)	0.107 70(3)
C(1)	0.023 7(22)	0.251 6(18)	0.236 3(15)
C(2)	–0.041 7(22)	0.200 7(19)	0.180 1(15)
C(3)	–0.021 0(19)	0.214 5(16)	0.091 4(13)
C(4)	0.013 0(26)	0.294 5(22)	0.059 5(18)
C(5)	–0.076 1(26)	0.147 1(21)	0.041 9(18)
C(6)	0.339 5(19)	0.047 0(16)	0.055 1(14)
C(7)	0.252 1(24)	–0.015 4(19)	0.073 0(16)
C(8)	0.232 2(20)	–0.032 6(16)	0.159 8(13)
C(9)	0.317 9(18)	–0.018 6(15)	0.219 7(13)
C(10)	0.144 5(24)	–0.089 2(20)	0.175 5(17)

straints after displacement of the alkene moieties by triphenylphosphine, they allow a coplanar arrangement of the two square-planar platinum(II) moieties with a common S...S vector.

Concordant with the existence of a centre of inversion, the two bridging thiolato groups have an *anti* conformation with respect to each other as expected on steric grounds and the iodine atoms are *trans* to each other across the complex. The Pt–S bond lengths are 2.367(3) Å, which are slightly longer than those in the folded precursor (see above), and longer than in

Table 5. Selected intramolecular bond lengths (Å) and angles (°) for $[\{\text{PtI}(\text{PPh}_3)(\text{SCH}_2\text{CH}_2\text{CMe}=\text{CH}_2)\}_2]$

I–Pt(1)	2.621(1)	S–Pt(1a)	2.367(3)
P–Pt(1)	2.267(3)	Pt(1)···Pt(1a)	3.539(1)
C(1)–S	1.831(7)	C(11)–P	1.825(6)
C(21)–P	1.827(6)	C(31)–P	1.813(6)
C(2)–C(1)	1.495(9)	C(3)–C(2)	1.495(9)
C(4)–C(3)	1.456(12)	C(5)–C(3)	1.332(12)
S–Pt(1)–I	89.2(1)	P–Pt(1)–I	92.0(1)
P–Pt(1)–S	178.0(1)	C(1)–S–Pt(1)	102.9(3)
C(11)–P–Pt(1)	113.3(2)	C(21)–P–Pt(1)	115.4(2)
C(21)–P–C(11)	102.4(3)	C(31)–P–Pt(1)	114.6(2)
C(31)–P–C(11)	106.6(3)	C(31)–P–C(21)	103.2(3)
C(2)–C(1)–S	114.7(5)	C(3)–C(2)–C(1)	114.7(6)
C(4)–C(3)–C(2)	117.8(8)	C(5)–C(3)–C(2)	119.7(9)
C(5)–C(3)–C(4)	122.5(9)		

Key to symmetry operation relating designated atom to reference atoms at (x, y, z): (a) –x, 1.0 –y, –z.

terminal thioether complexes, as for example in the cases of $[\text{PtBr}_2(\text{MeSCH}_2\text{CH}_2\text{CH}_2\text{CH}=\text{CH}_2)]^1$ and $[\text{PtI}_2\{\text{S}(\text{CH}_2\text{CH}_2\text{CH}=\text{CH}_2)_2\}]^2$ where the Pt–S bond lengths are 2.286(7) and 2.280(5) Å, respectively.

N.M.R. Studies.—Proton n.m.r. data for the complexes of types (1) and (2) are reported in Tables 7 and 8 respectively. The solid-state structures of all the complexes of type (1) are assumed to be analogous to that observed for $[\{\text{PtI}(\text{SCH}_2\text{CH}_2\text{CMe}=\text{CH}_2)\}_2]$ and those of the alkene-displaced derivatives of type (2) are assumed to be analogous to that of $[\{\text{PtI}(\text{PPh}_3)(\text{SCH}_2\text{CH}_2\text{CMe}=\text{CH}_2)\}_2]$.

Complexes containing chelating bridging alkenyl chalcogenato ligands. N.m.r. studies on $[\{\text{PtX}(\text{ECH}_2\text{CH}_2\text{CMe}=\text{CH}_2)\}_2]$ (X = Cl, Br, or I; E = S or Se) indicate that there is only one solution-state geometry and that this geometry is consistent with the structural data from the X-ray analysis. The ^1H n.m.r. spectrum shows only co-ordinated alkenic protons for which $^2J(^1\text{H}-^{195}\text{Pt}) \approx 70$ Hz. In the dialkenylchalcogenoether precursor to the dimeric complexes containing chelating bridging alkenyl chalcogeno ligands (*i.e.* before chalcogen dealkylation has occurred, see Scheme 1) a fluxional process, rapid at room temperature in solution, causes exchange of the two alkene moieties at the available co-ordination site of the metal (this process is described in detail in our earlier paper²) and results in the observation of averaged $^2J(^1\text{H}-^{195}\text{Pt})$ coupling constants of about 35 Hz. It is therefore evident from n.m.r. spectroscopy after chalcogen dealkylation that the alkene-exchange process is no longer occurring, and that the alkene groups co-ordinated to platinum are static. The n.m.r. spectrum did not alter throughout the temperature range of –90 to +110 °C, showing also that the chelate effect constrains the ring too rigidly to permit pyramidal inversion at sulphur or selenium.

Complexes containing non-chelating bridging alkenyl chalcogenato ligands. In contrast to the above studies, n.m.r. studies on the derivatives obtained by treating complexes containing chelating alkenylthiolato and alkenylselenato ligands with phosphine or arsine ligands, *i.e.* $[\{\text{PtI}(\text{L})(\text{ECH}_2\text{CH}_2\text{CMe}=\text{CH}_2)\}_2]$ [L = PPh_3 , PPh_2Me , or $\text{As}(\text{CH}_2\text{SiMe}_3)_3$; E = S or Se], showed only the presence of unco-ordinated alkene moieties. From variable-temperature n.m.r. studies at least two dynamic processes appear to occur in solution. At low temperature (–90 °C) there are two sets of methylene proton signals (one for the *syn* and one for the *anti* conformers), arising from the two possible configurations at the two pyramidal chalcogen atoms (resonances at δ 3.24 and 3.65 for the complex $[\{\text{PtI}(\text{PPh}_3)-$

Table 6. Fractional atomic co-ordinates ($\times 10^4$) for $[\{\text{PtI}(\text{PPh}_3)(\text{SCH}_2\text{CH}_2\text{CMe}=\text{CH}_2)\}_2]\cdot\text{CHCl}_3$

Atom	x	y	z	Atom	x	y	z
Pt(1)	10 783.1(2)	4 782.6(2)	1 163.5(1)	C(24)	15 745(4)	10 096(3)	1 431(2)
I	9 717.2(4)	2 889.5(4)	2 392.4(3)	C(25)	15 107(4)	9 865(3)	2 332(2)
S	8 625.5(13)	2 730.0(12)	74.8(9)	C(26)	14 256(4)	8 569(3)	2 569(2)
P	12 894(1)	5 791(1)	2 159(1)	C(31)	12 708(4)	5 910(5)	3 493(3)
C(1)	8 723(6)	2 253(5)	-448(4)	C(32)	13 634(4)	5 745(5)	4 229(3)
C(2)	10 012(7)	2 530(6)	-999(5)	C(33)	13 492(4)	5 916(5)	5 247(3)
C(3)	10 124(8)	1 323(7)	-1 387(6)	C(34)	12 423(4)	6 253(5)	5 528(3)
C(4)	9 015(14)	444(13)	-2 158(11)	C(35)	11 497(4)	5 418(5)	4 791(3)
C(5)	11 199(12)	1 074(12)	-1 011(11)	C(36)	11 639(4)	6 246(5)	3 774(3)
C(11)	14 074(3)	4 995(3)	2 027(3)	C(6)	1 863(44)	541(43)	4 732(31)
C(12)	13 484(3)	3 645(3)	1 736(3)	C(61)	3 067(24)	1 422(22)	5 289(16)
C(13)	14 382(3)	3 030(3)	1 642(3)	Cl(1)	2 382(9)	2 050(9)	4 444(7)
C(14)	15 870(3)	3 765(3)	1 838(3)	Cl(11)	2 047(15)	2 284(13)	5 012(11)
C(15)	16 460(3)	5 115(3)	2 130(3)	Cl(2)	1 938(9)	952(9)	6 331(7)
C(16)	15 562(3)	5 730(3)	2 224(3)	Cl(21)	1 797(14)	-1(13)	6 014(10)
C(21)	14 043(4)	7 505(3)	1 904(2)	Cl(3)	3 665(12)	596(11)	4 649(8)
C(22)	14 681(4)	7 736(3)	1 003(2)	Cl(31)	2 732(18)	-245(16)	4 955(12)
C(23)	15 531(4)	9 032(3)	767(2)				

Table 7. Proton n.m.r. data* for complexes $[\{\text{PtX}(\text{ECH}_2\text{CH}_2\text{CMe}=\text{CH}_2)\}_2]$

Sample	$\delta(\text{H}_a)$	$\delta(\text{H}_b)$	$\delta[\text{H}(\text{Me})]$	$^2J(\text{H}_a-\text{Pt})$	$^2J(\text{H}_b-\text{Pt})$	$^3J[\text{H}(\text{Me})-\text{Pt}]$
$[\{\text{PtCl}(\text{SCH}_2\text{CH}_2\text{CMe}=\text{CH}_2)\}_2]$	4.52	4.17	2.20	64.5	66.4	36.7
$[\{\text{PtBr}(\text{SCH}_2\text{CH}_2\text{CMe}=\text{CH}_2)\}_2]$	4.66	4.19	2.28	66.4	66.5	37.5
$[\{\text{PtI}(\text{SCH}_2\text{CH}_2\text{CMe}=\text{CH}_2)\}_2]$	4.91	4.24	2.42	69.1	68.4	38.2
$[\{\text{PtCl}(\text{SeCH}_2\text{CH}_2\text{CMe}=\text{CH}_2)\}_2]$	5.17	4.78	2.00	63.2	59.2	38.2
$[\{\text{PtBr}(\text{SeCH}_2\text{CH}_2\text{CMe}=\text{CH}_2)\}_2]$	5.17	4.80	2.23	62.8	57.8	38.0
$[\{\text{PtI}(\text{SeCH}_2\text{CH}_2\text{CMe}=\text{CH}_2)\}_2]$	4.87	4.26	2.27	70.5	68.6	38.2

* Shifts (δ) and coupling constants (J in Hz) measured in CDCl_3 . Alkene protons H_a and H_b assigned *trans* and *cis* to alkenic methyl group, respectively.

Table 8. Proton n.m.r. data^a for the complexes $[\{\text{PtI}(\text{L})(\text{ECH}_2\text{CH}_2\text{CMe}=\text{CH}_2)\}_2]$

Sample	$\delta(\text{H}_a)$	$\delta(\text{H}_b)$	$\delta[\text{H}(\text{Me})]$	$\delta[\text{H}(\text{ECH}_2)]$
$[\{\text{PtI}(\text{PPh}_3)(\text{SCH}_2\text{CH}_2\text{CMe}=\text{CH}_2)\}_2]$	4.70	4.56	1.70	3.36
$[\{\text{PtI}(\text{PPh}_2\text{Me})(\text{SCH}_2\text{CH}_2\text{CMe}=\text{CH}_2)\}_2]$	4.67 ^b	4.56 ^b	1.66	3.12
$[\{\text{PtI}[\text{As}(\text{CH}_2\text{SiMe}_3)_3](\text{SCH}_2\text{CH}_2\text{CMe}=\text{CH}_2)\}_2]$	4.77 ^c	4.77 ^c	1.74	3.00
$[\{\text{PtI}(\text{PPh}_3)(\text{SeCH}_2\text{CH}_2\text{CMe}=\text{CH}_2)\}_2]$	4.75	4.68	1.75	3.06
$[\{\text{PtI}[\text{As}(\text{CH}_2\text{SiMe}_3)_3](\text{SeCH}_2\text{CH}_2\text{CMe}=\text{CH}_2)\}_2]$	4.81 ^b	4.77 ^b	1.71	2.90

^a Shifts (δ) measured in CDCl_3 ; values quoted at fast chalcogen inversion. Alkene protons H_a and H_b assigned *trans* and *cis* to alkenic methyl group, respectively. ^b Major isomer. ^c Not clearly assignable.

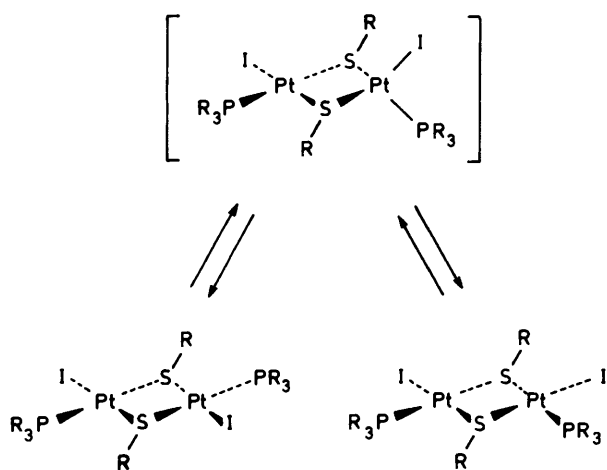
Table 9. Data from n.m.r. coalescence-temperature studies

Complex	Coalescing protons	Chemical shift difference between coalescing protons of static state (Hz)	Coalescence temperature, T_c/K	$\Delta G^\ddagger T_c^*$ kJ mol^{-1}
$[\{\text{PtI}(\text{PPh}_3)(\text{SCH}_2\text{CH}_2\text{CMe}=\text{CH}_2)\}_2]$	ECH_2	102	273	54.4
$[\{\text{PtI}[\text{As}(\text{CH}_2\text{SiMe}_3)_3](\text{SCH}_2\text{CH}_2\text{CMe}=\text{CH}_2)\}_2]$	Alkene	26.7	260	54.6
$[\{\text{PtI}(\text{PPh}_3)(\text{SeCH}_2\text{CH}_2\text{CMe}=\text{CH}_2)\}_2]$	ECH_2	62.2	333	68.2
$[\{\text{PtI}[\text{As}(\text{CH}_2\text{SiMe}_3)_3](\text{SeCH}_2\text{CH}_2\text{CMe}=\text{CH}_2)\}_2]$	Alkene	27	310	65.5

* Error $\approx \pm 1 \text{ kJ mol}^{-1}$.

$(\text{SCH}_2\text{CH}_2\text{CMe}=\text{CH}_2)_2$). As the temperature is raised, these signals coalesce as exchange occurs between the two conformers *via* chalcogen inversion, until at $+30^\circ\text{C}$ fast exchange occurs and a single average signal is observed at δ 3.36. For complexes with Pt-S-Pt-S rings another fluxional process may occur in solution, *viz.* ring reversal. This process may occur, however, only in complexes which contain a non-planar ring. In the present cases, the Pt_2S_2 rings of the complexes of Type (2) are planar in the solid state and either retain planarity in solution or the reversal process is fast at the temperatures at which the

spectra were recorded, as the spectra do not suggest a rationale to the contrary. The energy barriers (see Table 9) were determined from coalescence in the methylene proton region for the phosphine complexes, and for the arsine complexes were determined from coalescence in the alkene proton region, since these protons also appear to be sensitive to the configuration at sulphur and are rendered equivalent by the inversion process. The dynamic n.m.r. characteristics, coalescence temperatures, and energy barriers for the arsine complexes are very similar to those of the analogous phosphine complexes despite the



Scheme 2.

considerable difference between PPh_3 and $\text{As}(\text{CH}_2\text{SiMe}_3)_3$. The characteristics of the selenato-bridged complexes are similar to those of the analogous thiolato-bridged complexes, but the coalescence temperatures are observed to be higher and the energy barriers are greater by about 10 kJ mol^{-1} . Such a difference is usually observed in comparative inversion studies of these two elements⁹ and is thought to be a result of the more effective orbital overlap in the planar transition state between the metal and sulphur than that between the metal and selenium.

Although the quantitative analysis of the pyramidal atomic inversion process may be carried out by complete bandshape analysis to determine the activation free energy, ΔG^\ddagger , at any temperature by evaluating both ΔH^\ddagger and ΔS^\ddagger , this method is difficult to implement where signals in the n.m.r. spectrum overlap or are particularly complex. Under such circumstances, as was the case with our studies, a less rigorous, but still useful alternative method may be used to evaluate ΔG^\ddagger at the coalescence temperature (T_c) only. The $\Delta G^\ddagger T_c$ energy values for the complexes are in Table 9 and were obtained according to this latter method and by use of the Eyring equation.

The $^{31}\text{P}\{-^1\text{H}\}$ n.m.r. spectra of the complexes $[\{\text{Pt}(\text{L})(\text{E}(\text{CH}_2\text{CH}_2\text{CMe}=\text{CH}_2)_2)\}_2]$ showed two phosphorus signals (15.82 and 17.94 p.p.m.), the relative intensities of which varied as a function of both temperature and time. These observations are consistent with the part isomerisation of the complex from *trans* to *cis* and subsequent establishment of a temperature-dependent equilibrium between the two. The isomerisation evidently passes through a relatively high-energy transition state because the exchange occurs at a rate too slow to be measurable by n.m.r. spectroscopy (not visible as line-broadening in the spectrum). This is consistent with an intramolecular 'pancake-flip' mechanism for the process, such as has been observed in some rhodium(I)¹⁶ and some palladium(II)¹⁷ complexes, which would involve a 180° rotation of one $\text{PtI}(\text{PR}_3)$ moiety relative to the rest of the complex. This mechanism would involve isomerisation *via* a transition state such as that shown in Scheme 2 wherein the rotating $\text{PtI}(\text{PR}_3)$ moiety attains a tetrahedral local geometry. Summerville and Hoffmann¹⁸ have shown that whether the ground-state structures of such bridged dimeric complexes contain tetrahedral or square-planar metal fragments is determined largely by the π -donor or π -acceptor capabilities of the bridging ligands. The attainment of such a 'pancake-flip' transition state as proposed in Scheme 2 may be greatly facilitated by the occurrence of rapid chalcogen inversion.

Although the geometry proposed for the above transition state has not been observed as the ground-state structure for

dinuclear d^8 metal complexes containing bridging chalcogenato groups, it is pertinent to note that the isoelectronic complex $[\text{Ir}_2(\mu\text{-PPh}_2)_2(\text{CO})_2(\text{PPh}_3)_2]$ ¹⁹ contains tetrahedrally coordinated edge-sharing metal moieties in the solid state. Summerville and Hoffmann¹⁸ have clearly shown that the interconversion of square-planar and tetrahedral co-ordination spheres involves a forbidden level crossing. Although this is consistent with the high activation energy expected for the isomerisation process, we cannot totally rule out other possible pathways, such as fission of one Pt-S bond, followed by rotation of the $\text{PtI}(\text{PR}_3)$ fragment about the remaining Pt-S bond.

In conclusion, it is clear that the chemical properties of chalcogenoether and chalcogenato complexes are significantly modified by the presence of the chelating alkenyl group. The C-S and C-Se bond cleavage in complexes of the type $[\text{PtX}_2\{\text{E}(\text{CH}_2\text{CH}_2\text{CMe}=\text{CH}_2)_2\}]$ is dramatically enhanced, whilst the chalcogen inversion process in $[\{\text{PtI}(\text{E}(\text{CH}_2\text{CH}_2\text{CMe}=\text{CH}_2)_2)\}_2]$ ⁹ is completely inhibited. The alkenic methyl group appears to play a crucial, though as yet unascertained, role in the chalcogen-dealkylation process, since even prolonged refluxing of the complexes $[\text{PtX}_2\{\text{E}(\text{CH}_2\text{CH}_2\text{CR}=\text{CR}'_2)_2\}]$ with an excess of lithium halide in a refluxing acetone solution did not result in dealkylation in the cases where $\text{R} = \text{R}' = \text{H}$ or where $\text{R} = \text{H}$ and $\text{R}' = \text{Me}$.

Experimental

General.—Reactions were carried out using standard Schlenk techniques under an atmosphere of dry nitrogen and solvents were dried and distilled under nitrogen before use (although the products are not noticeably sensitive to either air or water). The ligands 2,8-dimethyl-5-chalcogenanona-1,8-diene were prepared from the reaction between 4-mesyl-2-methyl-but-1-ene $\text{MeSO}_2\text{CH}_2\text{CH}_2\text{CMe}=\text{CH}_2$ (prepared from the corresponding alcohol) and the sodium chalcogenide according to previously detailed procedures.² Reaction of these ligands with potassium tetrachloroplatinate(II) yields the bidentate dialkenylchalcogenoether chelate complexes $[\text{PtCl}_2\{\text{E}(\text{CH}_2\text{CH}_2\text{CMe}=\text{CH}_2)_2\}]$, the precursors to the present series of complexes, following previous methods.²

Preparations.— $[\{\text{PtI}(\text{SCH}_2\text{CH}_2\text{CMe}=\text{CH}_2)_2\}_2]$ by *S*-dealkylation. To a warm (56°C) stirring solution of $[\text{PtCl}_2\{\text{S}(\text{CH}_2\text{CH}_2\text{CMe}=\text{CH}_2)_2\}]$ (0.500 g, 1.147 mmol) in acetone (25 cm^3) was added a solution of 3 equivalents of lithium iodide (0.461 g, 3.440 mmol) in acetone (5 cm^3). The solution was refluxed gently for 1 h. During this time the colour darkened from pale yellow to deep red. The solution was cooled to room temperature and then filtered from the precipitate (LiCl) and the solvent removed under reduced pressure. The dark red product was washed with hexane several times and recrystallised from a chloroform-hexane two-layer system (yield 0.170 g, 35%).

Bromo- and chloro-derivatives. These were obtained by a similar method to the iodo-derivative above by addition of the appropriate lithium halide, but in poorer yields and required refluxing in acetone for 1–3 h.

Selenium derivatives. The selenium complexes were obtained analogously to the sulphur complexes but in slightly greater yield with shorter reaction times.

$[\{\text{PtI}(\text{PPh}_3)(\text{SCH}_2\text{CH}_2\text{CMe}=\text{CH}_2)_2\}_2]$ by alkene displacement. To a stirred solution of the chelate-bridged dimeric precursor $[\{\text{PtI}(\text{SCH}_2\text{CH}_2\text{CMe}=\text{CH}_2)_2\}]$ (0.200 g, 0.162 mmol) in chloroform (15 cm^3) was added slowly a solution of 2 equivalents of triphenylphosphine (0.085 g, 0.323 mmol) in chloroform (5 cm^3). An immediate reaction occurred and the colour became yellow. After stirring for a further 20 min hexane was added to induce virtually quantitative crystallisation of the product (0.274 g, 96%).

Table 10. Crystal data and details of intensity measurements for $[\{\text{Pt}(\text{SCH}_2\text{CH}_2\text{CMe}=\text{CH}_2)_2\}_2]$

Formula	$\text{C}_{10}\text{H}_{18}\text{I}_2\text{Pt}_2\text{S}_2$
<i>M</i>	846.8
Crystal system	Orthorhombic
Space group	<i>Pbca</i>
<i>a</i> /Å	12.733(3)
<i>b</i> /Å	15.288(2)
<i>c</i> /Å	16.904(3)
<i>U</i> /Å ³	3 277.3
<i>Z</i>	8
<i>D</i> _c /g cm ⁻³	3.43
<i>F</i> (000)	2 975
Crystal size/mm	0.2 × 0.2 × 0.2
$\mu(\text{Mo-K}\alpha)/\text{cm}^{-1}$	201.45

Table 11. Crystal data and details of intensity measurements for $[\{\text{Pt}(\text{PPh}_3)(\text{SCH}_2\text{CH}_2\text{CMe}=\text{CH}_2)_2\}_2]\cdot\text{CHCl}_3$

Formula	$\text{C}_{47}\text{H}_{49}\text{Cl}_3\text{I}_2\text{P}_2\text{Pt}_2\text{S}_2$
<i>M</i>	1 490.27
Crystal system	Triclinic
Space group	<i>P</i> $\bar{1}$
<i>a</i> /Å	10.396(1)
<i>b</i> /Å	11.250(5)
<i>c</i> /Å	13.348(2)
α /°	91.63(3)
β /°	94.53(1)
γ /°	116.02(3)
<i>U</i> /Å ³	1 395.0
<i>Z</i>	1
<i>D</i> _c /g cm ⁻³	1.77
<i>F</i> (000)	757
$\mu(\text{Mo-K}\alpha)/\text{cm}^{-1}$	62.65

Selenium analogues and of other phosphine and arsine derivatives. These complexes were prepared analogously to the sulphur complex above. The tris(trimethylsilylmethyl)arsine complexes, however, being much more soluble, were crystallised from a concentrated hexane solution at -20°C .

N.M.R. Studies.—Proton n.m.r. experiments were performed using a Brüker AM250 spectrometer operating at 250 MHz, using CD_2Cl_2 as solvent at low temperature, $\text{CDCl}_2\text{CDCl}_2$ at high temperature, and CDCl_3 whenever the temperature range was suitable.

Crystal Structure Determination of $[\{\text{Pt}(\text{SCH}_2\text{CH}_2\text{CMe}=\text{CH}_2)_2\}_2]$.—Crystals were grown from a two-layer liquid system of hexane over a chloroform solution of the complex. Crystal data are given in Table 10 and details of the structure refinement are summarised below.

Data collection. Crystal data were obtained using a Hilger and Watts Y290 automatic four-circle diffractometer with graphite-monochromated $\text{Mo-K}\alpha$ radiation. A total of 1 530 unique reflections were collected ($2 < \theta < 22^\circ$). The segment of reciprocal space scanned was *h* 0–13, *k* 0–16, *l* 0–8. The reflection intensities were corrected for absorption using the DIFABS method,²⁰ maximum and minimum transmission factors were 1.67 and 0.73 respectively.

Structure solution and refinement. The structure was solved by a Patterson search (SHELX 86²¹) and refined by full-matrix least squares (SHELX 76²²). The platinum, sulphur, and iodine atoms were refined anisotropically; the carbon atoms were refined isotropically. The final residual *R* was 0.41 (unit weights) for the 95 variables and 1 530 data for which $F_o > 3\sigma(F_o)$. A final electron-density difference synthesis showed a maximum peak of $1.22 \text{ e } \text{Å}^{-3}$.

Atomic scattering factors and anomalous dispersion parameters were taken from refs. 23 and 24, respectively.

Crystal structure determination of $[\{\text{Pt}(\text{PPh}_3)(\text{SCH}_2\text{CH}_2\text{CMe}=\text{CH}_2)_2\}_2]$.—Crystals suitable for X-ray analysis were grown from a two-layer liquid system of hexane over a chloroform solution of the complex. The crystal data are given in Table 11 and details of the intensity measurements and structure refinement are summarised below.

Data collection. Unit-cell parameters and intensity data were obtained by following previously detailed procedures,²⁵ using a CAD4 diffractometer operating in the ω – 2θ scan mode, with graphite-monochromated $\text{Mo-K}\alpha$ radiation. A total of 4 899 unique reflections were collected ($1.5 < \theta < 25.0^\circ$). The segment of reciprocal space scanned was *h* – 12 to 12, *k* – 13 to 13, *l* 0–15. The reflection intensities were corrected for absorption by semiempirical methods; maximum transmission factor 99.8%, minimum 33.3%.

Structure solution and refinement. The structure was solved by the application of routine heavy-atom methods and refined using full-matrix least-squares methods.²⁶ Phenyl groups were treated as rigid hexagons (C–C 1.395 Å, C–C–C 120°) with hydrogen atoms included at fixed distances (C–H 0.96 Å). The final residuals *R* and *R'* were 0.027 and 0.040 respectively for the 261 variables and 4 412 data for which $F_o > 3\sigma(F_o)$. The weighting scheme used was $w = 1/[\sigma^2(F_o) + 0.0008 F_o^2]$. Scattering factors were taken from ref. 27 and computations were performed using a DEC VAX-11/750 computer.

Additional material available from the Cambridge Crystallographic Data Centre comprises H-atom co-ordinates, thermal parameters, and remaining bond angles.

References

- E. W. Abel, P. A. Bates, D. G. Evans, M. B. Hursthouse, J. R. Koe, and V. Sik, *J. Chem. Soc., Dalton Trans.*, 1989, 985.
- E. W. Abel, P. A. Bates, D. G. Evans, M. B. Hursthouse, J. R. Koe, and V. Sik, *J. Chem. Soc., Dalton Trans.*, 1989, 2315.
- P. Klason, *Chem. Ber.*, 1895, **28**, 1493.
- R. G. Hayter, *Prep. Inorg. React.*, 1965, **2**, 211.
- T. Boschi, B. Crociani, L. Toniollo, and U. Belluco, *Inorg. Chem.*, 1970, **9**, 532.
- T. B. Rauchfuss, J. S. Shu, and D. M. Roundhill, *Inorg. Chem.*, 1976, **15**, 2096.
- E. W. Abel, R. P. Bush, F. J. Hopton, and C. R. Jenkins, *Chem. Commun.*, 1966, 58.
- P. Haake and P. C. Turley, *J. Am. Chem. Soc.*, 1967, **89**, 4611.
- E. W. Abel, S. K. Bhargava, and K. G. Orrell, *Prog. Inorg. Chem.*, 1984, **32**, 1.
- J. Chatt and F. A. Hart, *J. Chem. Soc.*, 1960, 2807.
- C. W. Blomstrand, *J. Prakt. Chem.*, 1883, **27**, 161.
- S. G. Murray and F. R. Hartley, *Chem. Rev.*, 1981, **81**, 365.
- T. A. Albright, R. Hoffmann, J. C. Thibault, and D. L. Thorn, *J. Am. Chem. Soc.*, 1979, **101**, 3801.
- C. E. Briant, C. J. Gardner, T. S. A. Hor, N. D. Howells, and D. M. P. Mingos, *J. Chem. Soc., Dalton Trans.*, 1984, 2645.
- T. Blake-Vance, L. G. Warner, and K. Seff, *Inorg. Chem.*, 1977, **16**, 2106.
- R. Hill, B. A. Kelly, F. G. Kennedy, S. A. R. Knox, and P. Woodward, *J. Chem. Soc., Chem. Commun.*, 1977, 434.
- E. W. Abel, N. A. Cooley, K. Kite, K. G. Orrell, V. Sik, M. B. Hursthouse, and H. M. Dawes, *Polyhedron*, 1987, **6**, 1261.
- R. H. Summerville and R. Hoffmann, *J. Am. Chem. Soc.*, 1976, **98**, 7240.
- R. Mason, I. Sotofte, S. D. Robinson, and M. F. Uttley, *J. Organomet. Chem.*, 1972, **46**, C61.
- D. Stuart and N. Walker, *Acta Crystallogr., Sect. A*, 1983, **39**, 158.
- G. M. Sheldrick, SHELX 86 Program for Crystal Structure Solution, University of Göttingen, 1986.

- 22 G. M. Sheldrick, SHELX 76 Program for Crystal Structure Determination and Refinement, University of Cambridge, 1976.
- 23 D. T. Cromer and J. B. Mann, *Acta Crystallogr., Sect. A*, 1968, **24**, 321.
- 24 D. T. Cromer and D. Liberman, *J. Chem. Phys.*, 1970, **53**, 1891.
- 25 M. B. Hursthouse, R. A. Jones, K. M. A. Malik, and G. Wilkinson, *J. Am. Chem. Soc.*, 1979, **101**, 4128.
- 26 G. M. Sheldrick, SHELX program for Crystal Structure Determination, University of Göttingen, 1980.
- 27 P. G. Edwards, G. Wilkinson, M. B. Hursthouse, and K. M. A. Malik, *J. Chem. Soc., Dalton Trans.*, 1980, 2467.

Received 6th December 1989; Paper 9/05290I